PCCP

RSC Publishing

PAPER

View Article Online
View Journal | View Issue

Cite this: *Phys. Chem. Chem. Phys.*, 2013, **15**, 2210

Access to enhanced differences in Marcus–Hush and Butler–Volmer electron transfer theories by systematic analysis of higher order AC harmonics

Gareth P. Stevenson,[a] Ruth E. Baker,[b] Gareth F. Kennedy,[c] Alan M. Bond,*[c] David J. Gavaghan*[a] and Kathryn Gillow[d]

Received 11th September 2012,
Accepted 9th November 2012

DOI: 10.1039/c2cp43193a

www.rsc.org/pccp

The potential-dependences of the rate constants associated with heterogeneous electron transfer predicted by the empirically based Butler–Volmer and fundamentally based Marcus–Hush formalisms are well documented for dc cyclic voltammetry. However, differences are often subtle, so, presumably on the basis of simplicity, the Butler–Volmer method is generally employed in theoretical–experimental comparisons. In this study, the ability of Large Amplitude Fourier Transform AC Cyclic Voltammetry to distinguish the difference in behaviour predicted by the two formalisms has been investigated. The focus of this investigation is on the difference in the profiles of the first to sixth harmonics, which are readily accessible when a large amplitude of the applied ac potential is employed. In particular, it is demonstrated that systematic analysis of the higher order harmonic responses in suitable kinetic regimes provides predicted deviations of Marcus–Hush from Butler–Volmer behaviour to be established from a single experiment under conditions where the background charging current is minimal.

1 Introduction

In the 1950s and 1960s Marcus and Hush independently developed a detailed theory for homogeneous electron transfer reactions (see ref. 1–10), which, when applied to electrochemical heterogeneous electron transfer scenarios, overcame the problem that the Butler–Volmer formalism predicts rates of oxidation (and reduction) that grow without bound as the applied potential is increased. Chidsey restated the Marcus–Hush principles, using ideas introduced by Levich for dc voltammetry associated with heterogeneous electron transfer,[11] and offered a formalism that was fundamentally superior to the Butler–Volmer model.[12] Compton *et al.*[13–18] have reviewed progress in the electrochemical use of Marcus–Hush theory and introduced further extensions they term the asymmetric Marcus theory. This group, in their recent and very comprehensive papers on the subject,[13–18] have also provided dc and square wave experimental data to support theoretical work showing how distinctions in the Butler–Volmer and Marcus–Hush models may emerge.

In a series of papers, we and others,[19–23] have recently expanded the use of Fourier or Hibbert or other forms of transformed ac voltammetry relative to that introduced by Smith *et al.* in their pioneering studies[24–28] usually related to polarography (voltammetry at a dropping electrode). To date the Butler–Volmer description of electron transfer has been exclusively employed, even though it may be inadequate in some situations. Thus, we now introduce into the large amplitude FT-ac voltammetric method the more fundamentally based description of electron transfer kinetics that utilises Marcus–Hush theory.[1–10]

The key difference in predictions derived from the use of the Butler–Volmer and Marcus–Hush theories in their standard forms is related to the dependence of the electron transfer rate constants on potential. With Butler–Volmer theory, the rate constants increase exponentially as a function of the applied potential E relative to the reversible potential E^0 or $|E - E^0|$. In contrast, the Marcus–Hush theory predicts that, at sufficiently large values of $|E - E^0|$, the rate constants become independent of potential. This levelling-off effect is analogous to the "inversion region" in homogeneous reactions.[29–32]

Since it has been extremely hard to demonstrate experimentally the Marcus–Hush effect under dc voltammetric conditions, the

[a] *University of Oxford, Department of Computer Science, Wolfson Building, Parks Road, Oxford OX1 3QD, UK. E-mail: david.gavaghan@cs.ox.ac.uk*
[b] *Centre for Mathematical Biology, Mathematical Institute, University of Oxford, 24-29 St. Giles', Oxford OX1 3LB, UK*
[c] *School of Chemistry, Monash University, Clayton, Victoria 3800, Australia. E-mail: alan.bond@monash.edu*
[d] *Numerical Analysis, Mathematical Institute, University of Oxford, 24-29 St. Giles', Oxford OX1 3LB, UK*

mathematically simpler Butler–Volmer model is still almost universally adopted in theory–experiment comparisons. Nevertheless, theoretical aspects of Marcus–Hush kinetics in electrochemistry remain of considerable current interest.[13–18,33,34] Numerical solutions using this theory are now even included in commercial simulation packages such as DigiSim and DigiElch, so reasons not to employ the model on the basis of mathematical complexity are now of a lesser concern. Arguably, the immediate need is to introduce techniques that enhance differences in the sensitivity of predictions of the Marcus–Hush and Butler–Volmer models, relative to those known to be available under transient or steady-state dc methods. Our aim is to provide further methodology that should assist experimentalists wishing to pursue the consequences of the Marcus–Hush formalism.

2 The Marcus–Hush and Butler–Volmer reaction mechanisms

In this paper two different classes of electrochemical systems will be considered: one is that of surface-confined electron transfer; the other is that of a species diffusing in solution with electron transfer occurring at the solution–electrode interface. Theory relevant to the surface to the surface-confined case will be described in some detail below. For the diffusional case, the reader is referred to models discussed in previous publications[19–21] which can be adapted to the Marcus–Hush formalism in an analogous manner. By surface-confined we mean that the electroactive centres of interest are attached to the electrode or adsorbed and are not free to diffuse. The mechanism considered is the one electron process represented as follows,

$$\mathrm{A_a} \underset{k_{\mathrm{red}}}{\overset{k_{\mathrm{ox}}}{\rightleftharpoons}} \mathrm{B_a} + e^-, \tag{1}$$

where the electron transfer reaction of interest takes place on the electrode surface. In eqn (1) the subscript a denotes that the species is adsorbed onto the electrode and k_{ox} and k_{red} (s^{-1}) are the oxidative and reductive potential-dependent charge transfer rate constants which, according to the Marcus–Hush thory, adapted to the electrochemical scenario by Chidsey,[12] are given by

$$\frac{k_{\mathrm{ox}}}{k^0} = \frac{\int_{-\infty}^{\infty} \frac{\exp\left\{-\left(x-\frac{\lambda-e(E-E^0-R_{\mathrm{u}}I_{\mathrm{tot}})}{k_{\mathrm{B}}T}\right)^2\left(\frac{k_{\mathrm{B}}T}{4\lambda}\right)\right\}}{1+\exp(x)}\mathrm{d}x}{\int_{-\infty}^{\infty} \frac{\exp\left\{-\left(x-\frac{\lambda}{k_{\mathrm{B}}T}\right)^2\left(\frac{k_{\mathrm{B}}T}{4\lambda}\right)\right\}}{1+\exp(x)}\mathrm{d}x}, \tag{2}$$

$$\frac{k_{\mathrm{red}}}{k^0} = \frac{\int_{-\infty}^{\infty} \frac{\exp\left\{-\left(x-\frac{\lambda+e(E-E^0-R_{\mathrm{u}}I_{\mathrm{tot}})}{k_{\mathrm{B}}T}\right)^2\left(\frac{k_{\mathrm{B}}T}{4\lambda}\right)\right\}}{1+\exp(x)}\mathrm{d}x}{\int_{-\infty}^{\infty} \frac{\exp\left\{-\left(x-\frac{\lambda}{k_{\mathrm{B}}T}\right)^2\left(\frac{k_{\mathrm{B}}T}{4\lambda}\right)\right\}}{1+\exp(x)}\mathrm{d}x}. \tag{3}$$

Eqn (2) and (3) can be rearranged as follows (as derived by Y.-P. Liu and used by Feldberg[33]),

$$\frac{k_{\mathrm{ox}}}{k^0} = \frac{\exp\left\{\frac{e(E-E^0)}{2k_{\mathrm{B}}T}\right\}\int_{-\infty}^{\infty} \frac{\exp\left\{-\frac{k_{\mathrm{B}}T}{\lambda}\left[x+\frac{e(E-E^0)}{2k_{\mathrm{B}}T}\right]^2\right\}}{\cosh(x)}\mathrm{d}x}{\int_{-\infty}^{\infty} \frac{\exp\left\{-\frac{k_{\mathrm{B}}T}{\lambda}x^2\right\}}{\cosh(x)}\mathrm{d}x}, \tag{4}$$

$$\frac{k_{\mathrm{red}}}{k^0} = \frac{\exp\left\{\frac{-e(E-E^0)}{2k_{\mathrm{B}}T}\right\}\int_{-\infty}^{\infty} \frac{\exp\left\{-\frac{k_{\mathrm{B}}T}{\lambda}\left[x+\frac{e(E-E^0)}{2k_{\mathrm{B}}T}\right]^2\right\}}{\cosh(x)}\mathrm{d}x}{\int_{-\infty}^{\infty} \frac{\exp\left\{-\frac{k_{\mathrm{B}}T}{\lambda}x^2\right\}}{\cosh(x)}\mathrm{d}x}. \tag{5}$$

Eqn (4) and (5) when combined with theory presented below make it easier to deduce that the Nernst equation is obeyed when the process is reversible ($k^0 \rightarrow \infty$ case).

In eqn (2)–(5): $E(t)$ is the applied potential, which in ac voltammetry consists of a sinusoidal voltage superimposed on a linear ramp;[19] E^0 is the formal reversible potential; e is the magnitude of the charge on one electron (C); k_B is Boltzmann's constant (eV K^{-1}); T is the temperature (K); λ is the reorganisation energy (eV); k^0 is the formal charge transfer rate constant (s^{-1}) at E^0.

In contrast to the Marcus–Hush model, the Butler–Volmer treatment,[10] gives

$$\frac{k_{\mathrm{ox}}}{k^0} = \exp\left((1-\alpha)\frac{nF}{RT}[E-E^0]\right), \tag{6}$$

$$\frac{k_{\mathrm{red}}}{k^0} = \exp\left(\frac{-\alpha nF}{RT}[E-E^0]\right), \tag{7}$$

where F is Faraday's constant (C mol^{-1}), R is the universal gas constant (J mol^{-1} K^{-1}) and α is the charge transfer coefficient. If Ohmic drop is present, then this can be represented by the product of the uncompensated resistance (R_u) and the current (I_{tot}). Introduction of the IR_u drop into eqn (6) and (7) gives

$$\frac{k_{\mathrm{ox}}}{k^0} = \exp\left((1-\alpha)\frac{nF}{RT}[E-E^0-R_{\mathrm{u}}I_{\mathrm{tot}}]\right), \tag{8}$$

$$\frac{k_{\mathrm{red}}}{k^0} = \exp\left(\frac{-\alpha nF}{RT}[E-E^0-R_{\mathrm{u}}I_{\mathrm{tot}}]\right). \tag{9}$$

Uncompensated resistance can be introduced into the Marcus–Hush model in an analogous way to that in the Butler–Volmer formalism. Since I_{tot} is the total current, it represents the sum of the Faradaic, $I_f(t)$, and capacitive, $I_c(t)$, currents. Thus,

$$\begin{aligned} I_{\mathrm{tot}}(t) &= I_{\mathrm{f}}(t) + I_{\mathrm{c}}(t), \\ &= Fa\frac{\mathrm{d}\Gamma_{\mathrm{A}}}{\mathrm{d}t} + \frac{\mathrm{d}}{\mathrm{d}t}[C_{\mathrm{dl}}(E_{\mathrm{eff}})E_{\mathrm{eff}}]. \end{aligned} \tag{10}$$

Here, $C_{dl}(E_{eff})$ is the double layer capacitance, in $F\ cm^{-2}$, given as a function of the effective voltage ($E_{eff} = E - E^0 - I_{tot}R_u$), a is the area of the electrode in cm^2 and $\Gamma_A(t)$ and $\Gamma_B(t)$ represent the coverage of species A and B, respectively, on the electrode surface (mol cm^{-2}) at a given time t (s).

By the conservation of mass it follows that

$$\Gamma_A(t) + \Gamma_B(t) = \Gamma^*, \quad (11)$$

where Γ^* is a constant that represents the total coverage. The use of eqn (11) and the assumption of a Langmuir isotherm, in which interactions between adsorbed molecules are negligible and all adsorption sites are equivalent, allows the chemistry represented in eqn (1) to be expressed mathematically as

$$\frac{d\Gamma_A}{dt} = k_{red}(\Gamma^* - \Gamma_A) - k_{ox}\Gamma_A. \quad (12)$$

Provision of an initial condition for each of eqn (2), (3) and (12) enables the voltammetric problem to be solved numerically.

2.1 Non-dimensional variables

In terms of achieving computational efficiency, it is useful to translate the dimensional parameters into non-dimensional variables. As has been discussed elsewhere,[21,35] the problem identified above can be re-cast in terms of non-dimensional variables. Since the voltammetric problem being addressed requires a linear relationship between time t and the dc component of applied potential, E_{DC}, then the dimensionless parameter τ can be defined by

$$\tau = F(E_i + \nu t)/RT = FE_{DC}/RT, \quad (13)$$

and used to replace both of these dimensional variables, where E_i is the initial potential, ν is the scan rate and R, T and F have their usual meanings.

Similarly, in the non-dimensional format

$$\varepsilon^0 = \frac{F}{RT}E^0. \quad (14)$$

The sine wave amplitude, ΔE, is non-dimensionalised to obtain

$$\Delta\tau = \frac{F\Delta E}{RT}, \quad (15)$$

whilst the angular frequency, ω, becomes

$$\Omega = \frac{RT\omega}{F\nu}. \quad (16)$$

This definition ensures that

$$\Omega\tau = \omega t + FE_i\Omega/RT.$$

Since Ω and E_i are experimental parameters, their values can be selected. By choosing Ω to be any even multiple of π, and values of E_i such that FE_i/RT is an even integer, it follows that

$$\sin j\omega t = \sin j\Omega\tau, \quad j = 0,1,2,3,\ldots \quad (17)$$

This allows a non-dimensional version of the applied potential to be developed, using eqn (13)–(16), where $\varepsilon(\tau)$ is the non-dimensional applied potential

$$\varepsilon(\tau) = \varepsilon_{DC}(\tau) + \varepsilon_{AC}(t) = \tau + \Delta\tau\,\sin(\Omega\tau). \quad (18)$$

Following a similar pattern as above, non-dimensional versions of k_{ox}, k_{red} and Γ_A denoted by κ_{ox}, κ_{red} and θ, respectively, can be generated as follows:

$$\kappa_{ox} = \frac{k_{ox}}{k^0}; \quad (19)$$

$$\kappa_{red} = \frac{k_{red}}{k^0}; \quad (20)$$

$$\text{and } \theta = \frac{\Gamma_A}{\Gamma^*}. \quad (21)$$

The following definitions for the non-dimensional uncompensated resistance, R_u^*, total current, ι_{tot}, overpotential, η, and reorganisation energy, λ^*, were also introduced

$$R_u^* = \frac{F^3 a\Gamma^* \nu}{R^2T^2}R_u, \ \iota_{tot}(\tau) = \frac{RT}{F^2 a\Gamma^* \nu}I_{tot}, \quad (22)$$

$$\eta = \frac{e(E - E^0)}{k_BT} \text{ and } \lambda^* = \frac{\lambda}{k_BT}. \quad (23)$$

Using all the information above, and noting that the integrals in the Chidsey formulation of the Marcus–Hush theory and the Butler–Volmer relationship are already non-dimensional, both models can be written entirely in non-dimensional terms

$$\frac{d\theta}{d\tau} = \kappa_{red}(1 - \theta) - \kappa_{ox}\theta, \quad (24)$$

with θ prescribed at $\tau = 0$ and

$$\iota_{tot} = n\frac{d\theta}{d\tau} + \frac{d}{d\tau}[\gamma_{dl}(\varepsilon_{eff})\varepsilon_{eff}], \quad (25)$$

where the non-dimensionalisation of $C_{dl}(E_{eff})$ will depend on its specific functional form. Whilst all computations were undertaken using non-dimensional variables, plots and figures are frequently presented in terms of dimensioned parameters readily recognized by electrochemists in order to simplify understanding of data in terms of experiments relevant to parameters values.

2.2 A numerical solution algorithm

The numerical solution algorithm used to solve the equations above involves backward Euler discretisations of the time derivative.[36] When using the Marcus–Hush description of electron transfer kinetics we require an accurate and computationally efficient method for evaluating integrals of the form of eqn (19) and (20). These integrals can be written in the form

$$\int_{-\infty}^{\infty} \frac{\exp\left[-(x - \beta_1)^2\left(\frac{1}{4\lambda^*}\right)\right]}{1 + \exp(x)}dx, \quad (26)$$

where λ^* is a positive constant and β_1 depends on time but can be treated as a constant as far as the integration is concerned, by recomputing the integral for each value of β_1. The important features of the integrand are as follows: it is always positive; it has a single maximum; it decays very quickly as $|x|$ increases; and the maximum translates along the x axis as β_1 changes. In order for many of the traditional methods of integration to be computationally efficient, the position of the maximum of the

integrand must be tracked and this, along with the fact that the integral has to be evaluated many times (at least 2^{18} times due to the time resolution required), means that an efficient computational technique must be used in order to solve these problems on practical timescales. These complexities, that are absent from the Butler–Volmer formalism, are one of the main reasons for Marcus–Hush theory currently being underused in electrochemistry. Clearly, an algorithm that can evaluate these rate constants accurately and in a timely manner is of some importance.

The method we use to compute this integral is Gauss–Hermite quadrature which states the following

$$\int_{-\infty}^{\infty} e^{-x^2} f(x)dx \approx \sum_{i=1}^{k} w_i f(x_i), \quad (27)$$

where k is the number of sample points, x_i are the k roots of the Hermite polynomial, $H_k(x)$, where

$$H_k(x) = (-1)^k e^{x^2} \frac{d^k}{dx^k}\left(e^{-x^2}\right), \quad (28)$$

and

$$w_i = \frac{2^{k-1}k!\sqrt{\pi}}{k^2[H_{k-1}(x_i)]^2}, \quad \text{for } i = 1, \ldots, k, \quad (29)$$

all of which can be pre-computed. We found this method to be stable and accurate across the whole range of parameter space and our results compared well with other more traditional methods such as the composite trapezium rule.

3 Prediction of differences based on Marcus–Hush and Butler–Volmer models when using dc voltammetry

In the theoretical comparison of the predictions of models employing Marcus–Hush or Butler–Volmer theory, uncompensated resistance and capacitance are ignored. The dc voltammetric case has already been considered by a number of authors,[33,37] so only a brief review of this scenario is provided in this paper. In the dc situation, when RTk^0/Fv is large, it should be noted that the voltammetry using either model adheres to the prediction of the Nernst equation and it was verified that the simulations also comply with this expectation. It is only when RTk^0/Fv is much smaller that large differences in predictions of dc voltammograms based on the two models emerge.

Fig. 1 shows the dependence of κ_{ox} (k_{ox}/k^0) on oxidation (and reduction) as a function of potential (parameters given in figure caption). The top plot is generated using Butler–Volmer kinetics. Since this is a semi-log plot and k^0 is a constant (value at E^0), the straight line reveals that this model predicts that the rate constant k_{ox} will increase exponentially as long as the applied potential is increased.[33,37] The other four plots in Fig. 1 are generated using Marcus–Hush kinetics for four different values of λ and we can see clearly that limiting values for k_{ox}/k^0 and k_{red}/k^0 are predicted, where the limits depend on reorganisation energy. These data also reveal that if λ is large, then the two models converge, assuming $\alpha = 0.5$ in the Butler–Volmer case. However, if $\alpha \neq 0.5$, then there is no simulation based on the Chidsey formulation of Marcus–Hush theory that will become coincident with the Butler–Volmer model. In this case, an asymmetric model of the Marcus theory would have to form the basis of the comparison.[13–18]

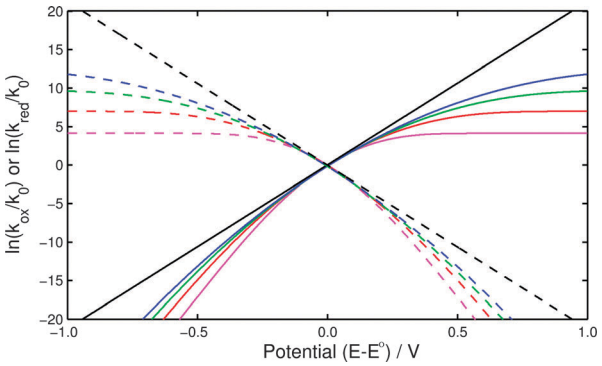

Fig. 1 Dependence of $\ln(k_{ox}/k_0)$ (solid lines) and $\ln(k_{red}/k_0)$ (dashed lines) on potential relative to E^0 under conditions of dc voltammetry for a surface-confined process with $k_0 = 1\ s^{-1}$. Black lines indicate Butler–Volmer kinetics with $\alpha = 0.5$. Blue, green, red and pink lines indicate Marcus–Hush kinetics with $\lambda = 1$, 0.75, 0.5, 0.25 eV, respectively. Other parameters: $a = 1\ cm^2$; $v = 1\ V\ s^{-1}$; $E^0 = 0$ V; $C_{dl} = 0\ F\ cm^{-2}$; $R_u = 0\ \Omega$; $k_0 = 1\ s^{-1}$; $T = 273$ K; and at $t = 0$ s, $\Gamma_A = 10$ pico-mol cm^{-2} and $\Gamma_B = 0$ pico-mol cm^{-2}.

Fig. 2 and 3 display predictions in the form of dc voltammograms as a function of k^0 when using Marcus–Hush kinetics for surface-confined and diffusing species, respectively. Fig. 2(a) and 3(a) show the effect of decreasing k^0, assuming Marcus–Hush

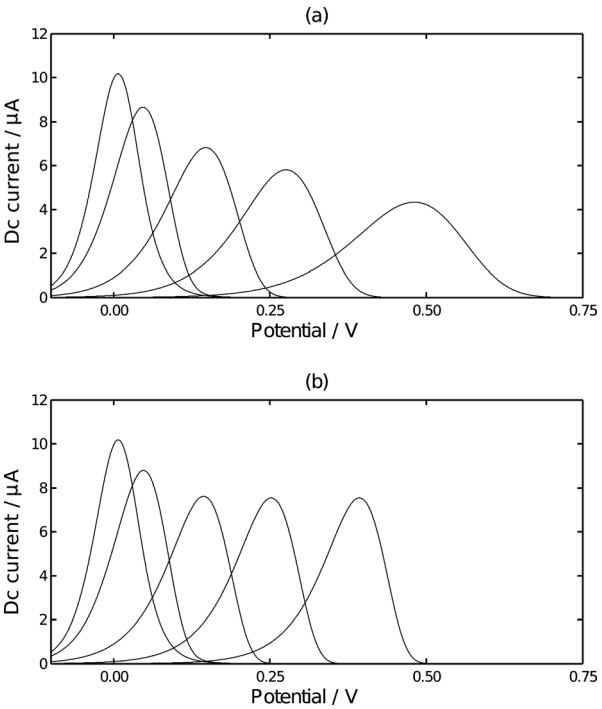

Fig. 2 Predicted dc voltammograms for a surface-confined species based on (a) Marcus–Hush with $\lambda = 0.85$ eV and (b) Butler–Volmer kinetics with $\alpha = 0.5$, as a function of k_0. Left to right $k_0 = 100$, 10, 1, 0.1, 0.005 s^{-1}. Other parameters: $a = 1\ cm^2$; $v = 1\ V\ s^{-1}$; $E^0 = 0$ V; $C_{dl} = 0\ F\ cm^{-2}$; $R_u = 0\ \Omega$; $T = 273$ K; and at $t = 0$ s, $\Gamma_A = 10$ pico-mol cm^{-2} and $\Gamma_B = 0$ pico-mol cm^{-2}.

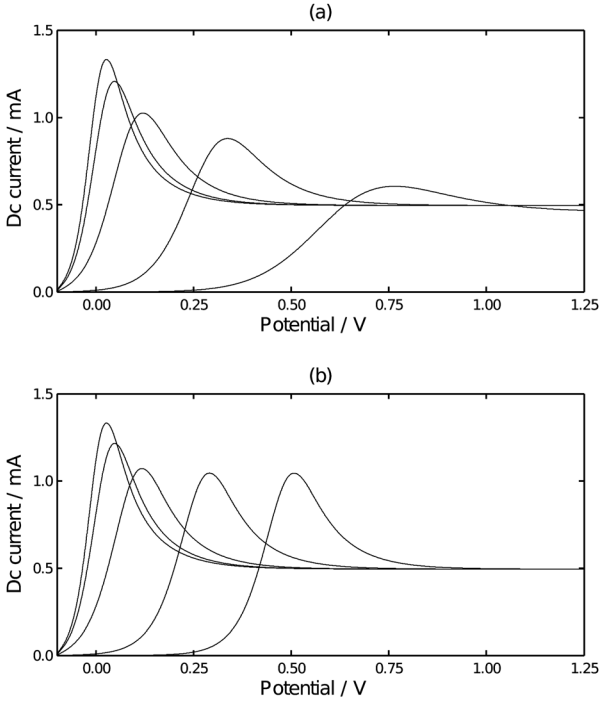

Fig. 3 Predicted dc voltammograms for a diffusing species based on (a) Marcus–Hush kinetics with λ = 0.85 eV and (b) Butler–Volmer kinetics with α = 0.5, as a function k_0. Left to right k_0 = 1 × 10^6, 1 × 10^4, 4 × 10^3, 300, 1 cm s^{-1}. Other parameters: a = 1 cm^2; v = 1 V s^{-1}; E^0 = 0 V; C_{dl} = 0 F cm^{-2}; R_u = 0 Ω; T = 273 K; and at t = 0 s, Γ^* = 10^{-6} mol cm^{-3} and D = 2.3 × 10^{-5} cm^2 s^{-1}.

kinetics apply: the peak current progressively decreases and the voltammetric wave-shape broadens. In contrast with Butler–Volmer kinetics in Fig. 2(b) and 3(b), the peak current drops initially as k^0 decreases, but then the peak current attains a constant value and the wave-shape becomes independent of k^0.[38]

4 Prediction of differences based on Marcus–Hush and Butler–Volmer models when using ac voltammetry

In Fourier-transformed (FT) ac voltammetry, the use of the FFT algorithm to convert data in the time domain to the frequency domain followed by band filtering and an application of the inverse FFT algorithm, as described elsewhere,[19–21,35] allows the dc and ac harmonics to be resolved. Essentially, the higher harmonics are more sensitive to k^0 than the dc or first harmonic and ideally they are also devoid of background capacitance. However, in order to simplify the presentation of results, uncompensated resistance and capacitance are again ignored in the simulations presented below. Importantly, it should be noted that all ac harmonic components are derived from a single experiment, whereas variation in the scan rate parameter that is critical in dc voltammetry requires a series of experiments to achieve the time dependence.

Fig. 4 shows peak current heights for the dc, first, third and fifth harmonic components for Butler–Volmer (in red) and Marcus–Hush (in black) kinetics across a range of $\xi = k^0/f$ values for a given scan rate of 1 V s^{-1}. The ac experiment has a dual time scale represented by the dc scan rate and the ac frequency. In this form of analysis, it is the ac frequency that is varied. Therefore the ac timescale is related to the order of the harmonics: higher harmonics refer to shorter timescales. In practice the upper frequency that is accessible is restricted by the maximum allowable frequency of the experimental instrumentation producing the ac signal. Nevertheless, Fig. 4 does convey regions where differences in the two models are predicted. The peak heights displayed in Fig. 4 are derived from the maximum value in each of the corresponding harmonics, and are easy to identify when the data is plotted as in Fig. 5. As is expected from consideration of the dc case described above, large ξ values, which imply the process is reversible, produce constant peak heights for each ac harmonic regardless of the formalism used. Again, this trivial result serves as a partial check that the solutions to the theory are sensible. The interesting divergence in the two theories is introduced when ξ is decreased, making the system quasi-reversible. In this regime Fig. 4, Butler–Volmer theory predicts that the ac peak heights tend to constant values, whereas Marcus–Hush theory predicts that the peak heights, across all harmonics, tend to zero as the system becomes progressively more irreversible (lower ξ values). Plots in Fig. 4 also indicate that the higher the harmonic, the more rapidly the peak height approaches zero (when decreasing ξ). Furthermore, and as expected, if the harmonic peak heights are plotted against $\kappa^0 = k^0RT/FV$ with a constant value of f = 30 Hz, analogous behaviour is observed to Fig. 4. Varying f over wide ranges is of course experimentally more tractable than varying v at constant f, as noted above.

These peak height patterns of behaviour provide us with a clear criterion for identifying Marcus–Hush behaviour. In ac voltammetric experimental data, as ξ is decreased, only if a levelling-off of the peak height occurs in each harmonic (more easily detected in the higher harmonics), is Butler–Volmer theory acceptable for describing the data.

Timmer and co-workers,[37] and later Smith and McCord,[39] also noted that when using the Butler–Volmer relationship in ac polarography (voltammetry at a dropping mercury electrode), ac currents do not decrease to zero as a process becomes less reversible. However, it does seem reasonable that if the rate constant approaches zero, then the ac current might be expected to approach zero; a feature provided by the Marcus–Hush model.

The peak height dependence may be translated into outcomes expected on the basis of full ac voltammetric analysis as a function of potential. Fig. 5 shows the voltammetric response for the dc, as well as first, third and fifth harmonic components with k^0 = 1 s^{-1} and other parameters given in the figure caption. In the dc voltammetric component, predictions based on the three models (Butler–Volmer with α = 0.5, Marcus–Hush with λ = 1 eV, and Marcus–Hush with λ = 0.25 eV) are difficult to distinguish, particularly when experimental error is considered. However, examination of the higher harmonics reveals that the differences in the predictions of the three models become increasingly evident. Fig. 6 shows the dc and ac harmonic components simulated using more irreversible kinetics (k^0 = 0.1 s^{-1}). Differences between Marcus–Hush and Butler–Volmer theories are now clearer, even in the dc component.

It is useful to now use parameter-sets in Chidsey's pioneering paper[12] for numerically simulating the voltammetry of a ferrocene

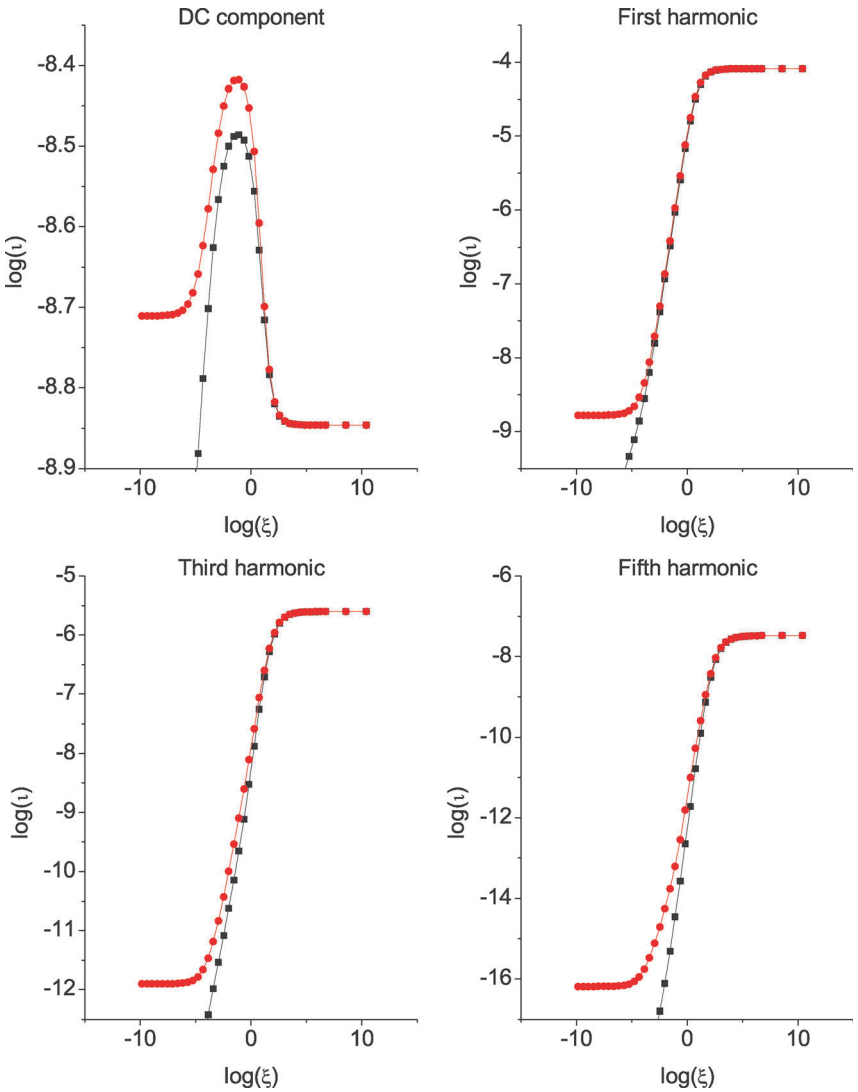

Fig. 4 Log–log plots of the non-dimensional peak current *versus* the non-dimensional parameter grouping $\xi = k_0/f$ for the dc component, first harmonic, third harmonic and fifth harmonic derived from FT-ac voltammetry. Black lines indicate Marcus–Hush theory with $\lambda = 0.25$ eV. Red lines indicate Butler–Volmer theory with $\alpha = 0.5$. Other parameters: $a = 1$ cm^2; $E^0 = 0$ V; $C_{dl} = 0$ F cm^{-2}; $R_u = 0$ Ω; $T = 273$ K; and at $t = 0$ s, $\Gamma_A = 10$ pico-mol cm^{-2} and $\Gamma_B = 0$ pico-mol cm^{-2}; $v = 1$ V s^{-1}; $\Delta E = 0.05$ V; and the potential was swept between −0.5 and 0.5 V.

group at a gold electrode using both Butler–Volmer and Marcus–Hush kinetics. This shows the benefits of using FT-ac voltammetry over dc voltammetry with experimentally relevant parameter values. In Fig. 7, simulated dc voltammograms are plotted with one parameter set used by Chidsey[12] (provided in the figure caption). As can be seen, differences in the Marcus–Hush and Butler–Volmer models are small when a scan rate of 0.5 V s^{-1} is used, and they would indeed be difficult to distinguish when experimental error is taken into account. In contrast, when FT-ac voltammetry is employed, as shown in Fig. 8, the two models are easily distinguishable for this experimentally realistic parameter-set.

Comparison of the theoretically derived data derived in Fig. 7 and 8 clearly demonstrate that harmonic analysis available in large amplitude ac voltammetry in principle provides a more sensitive probe of the applicability of either Marcus–Hush or Butler–Volmer theory to an experimental data set. A known limitation of the ac method is the low current magnitude obtained in the higher harmonics for the surface-confined model when the rate constant is small. As can be seen in the fifth harmonic in Fig. 5 and 6, the Marcus–Hush model gives a current magnitude of the order of 10^{-10} A, which is close to the experimental limit of measurement. This problem can be addressed to some extent by increasing the amplitude of the ac signal, ΔE, or by trying to increase the surface coverage of the electroactive species on the electrode. However, this measurability issue is clearly going to emerge at some higher harmonic order where the current will be too small to observe above experimental noise.

Fig. 9 compares the signal intensity of the fourth and fifth harmonics for the diffusional model ((a) and (b)) and the surface-confined model ((c) and (d)) for a set of parameters given in the figure caption. Clearly, the issues outlined in the paragraph above surrounding the signal intensities of higher harmonics are not as

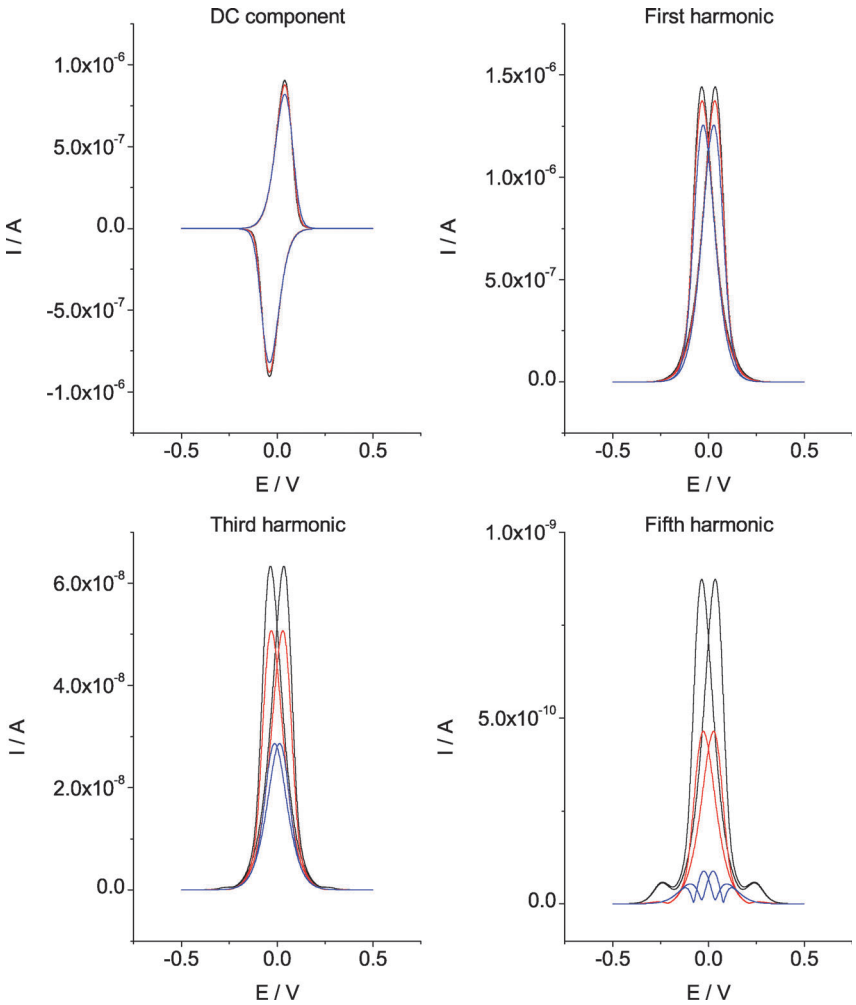

Fig. 5 Log–log plots of the non-dimensional peak current *versus* the non-dimensional parameter grouping $\kappa^0 = RTk_0/Fv$ for the dc component, first harmonic, third harmonic and fifth harmonic derived from FT-ac voltammetry. Black lines indicate Marcus–Hush theory with $\lambda = 0.25$ eV. Red lines indicate Butler–Volmer theory with $\alpha = 0.5$. Other parameters: $a = 1$ cm^2; $E^0 = 0$ V; $C_{dl} = 0$ F cm^{-2}; $R_u = 0$ Ω; $T = 273$ K; and at $t = 0$ s, $\Gamma_A = 10$ pico-mol cm^{-2} and $\Gamma_B = 0$ pico-mol cm^{-2}; $f = 30$ Hz; $\Delta E = 0.05$ V; and potential was swept between −0.5 and 0.5 V.

severe for the diffusional model. For example, in the fifth harmonic, the current response is of the order of 10^{-5} A for the diffusional model, compared with 10^{-10} A for the surface-confined model. This difference implies the problem of Ohmic (IR_u) drop will be more severe in the diffusive case. In surface-confined systems the current magnitude is usually of the order of hundreds of nano-amps, therefore the IR_u drop is unlikely to have a significant effect. However, in solution phase systems, where the current response is likely to be three or four orders of magnitude larger, IR_u drop often needs to be considered. Conversely, capacitance current can dominate dc voltammetry of surface-confined systems, but is not an issue in FT-ac voltammetry for the higher order harmonics.[36,40]

5 Implementation of Marcus–Hush model using the large amplitude FT-ac method

Given that the mathematical complexity of the Marcus–Hush model is no longer an issue, and because it utilises a more fundamental set of physical parameters, this model should be the natural choice to provide a description of electrode kinetics. It is useful therefore to consider how the Marcus–Hush model could be implemented when FT voltammetric ac data are available. A range of parameters may need to be deduced by simulation–experiment comparisons. However, ideally, as many parameters as possible should be measured independently so they can be classified as known. E^0 is usually known, but the determination of R_u and C_{dl} needs to be undertaken as both terms can produce distortion of the faradaic voltammetric characteristics. Assuming R_u and C_{dl} are accurately known and are included in the model as are electrode area, temperature, amplitude and frequency of the ac signal *etc.*, then the challenge is to provide unique values for k^0 and λ that fit the data over a wide time (or frequency) domain. In the dc voltammetric method, this requires undertaking a series of experiments over a range of scan rates, where the higher the scan rate, the more sensitive the response to k^0 and λ, but more problematic with regard to R_u and C_{dl} (solution soluble case). In the large-amplitude

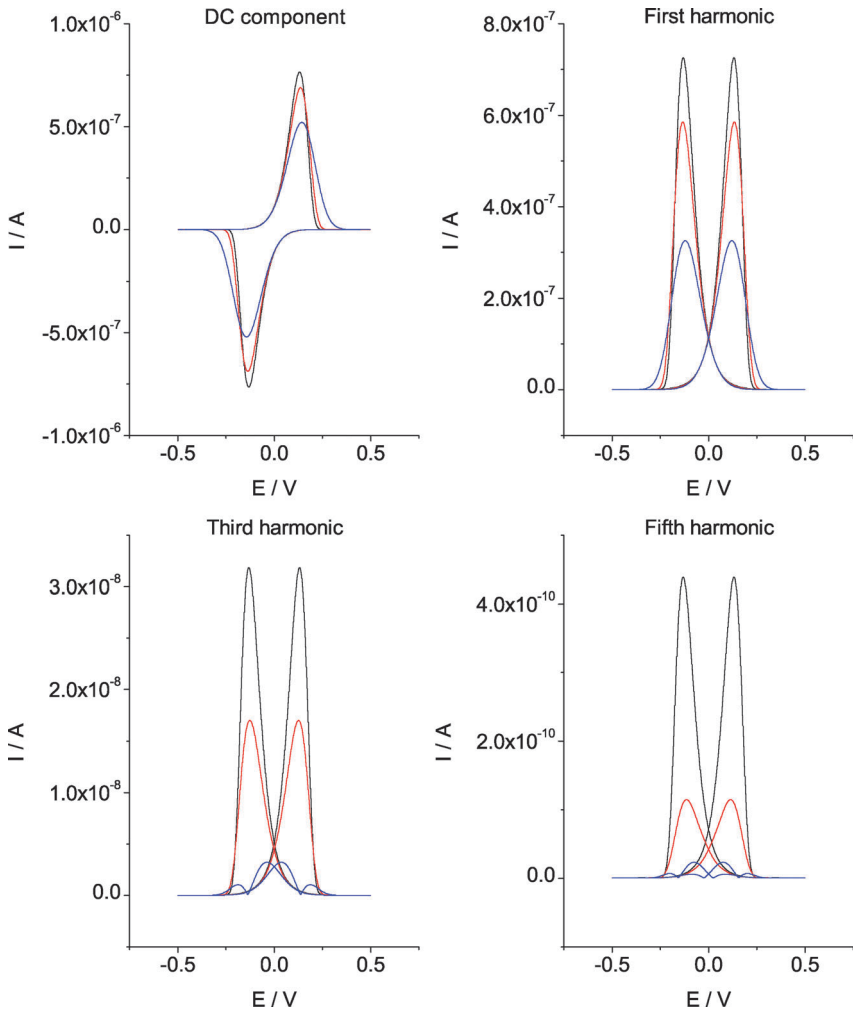

Fig. 6 Dc, first, third and fifth harmonic components derived from FT-ac voltammetry when $k_0 = 1\ s^{-1}$. Black lines indicate Butler–Volmer theory with $\alpha = 0.5$. Red lines indicate Marcus–Hush theory with $\lambda = 1$ eV. Blue lines indicate Marcus–Hush theory with $\lambda = 0.25$ eV. Other parameters: $a = 1\ cm^2$; $E^0 = 0$ V; $C_{dl} = 0\ F\ cm^{-2}$; $R_u = 0\ \Omega$; $T = 273$ K; and at $t = 0$ s, $\Gamma_A = 10$ pico-mol cm^{-2} and $\Gamma_B = 0$ pico-mol cm^{-2}; $f = 30$ Hz; $\Delta E = 0.05$ V; and $v = 0.1\ V\ s^{-1}$.

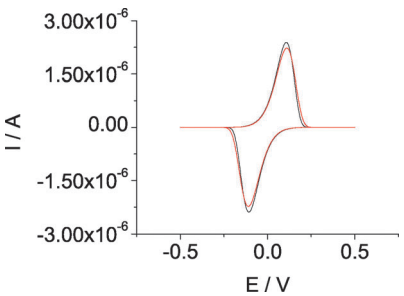

Fig. 7 Numerically simulated dc voltammograms using parameter-set taken from.[12] Black line indicates Butler–Volmer theory with $\alpha = 0.5$ and $k_0 = 1.25\ s^{-1}$. Red line indicates Marcus–Hush theory with $\lambda = 0.85$ eV and $k_0 = 1.295\ s^{-1}$. Other parameters: $a = 0.7\ cm^2$; $E^0 = 0$ V; $C_{dl} = 0\ F\ cm^{-2}$; $R_u = 0\ \Omega$; $T = 298$ K; and at $t = 0$ s, $\Gamma_A = 9.5$ pico-mol cm^{-2} and $\Gamma_B = 0$ pico-mol cm^{-2}; and $v = 0.5\ V\ s^{-1}$.

FT-ac approach, a single experiment in which a series of harmonics are available provides the analogous data set with the highest harmonics being most sensitive to k^0 and λ. R_u is also still important, but C_{dl} is ideally absent in the higher harmonics.

A more sophisticated approach available in FT-ac voltammetry is to apply a number of sine waves encompassing a range of frequencies rather than a single sine wave, so that even more data are available for the fundamental or higher harmonics, again will data obtained from a single experiment.[40] Finally, with the ac method, the scan rate also can be varied in a series of experiments.

Clearly, in the reversible limit, both theories converge to predictions based on the Nernst relationship. In the near reversible regime, the Butler–Volmer model is insensitive to α and k^0 and both are difficult to determine accurately; a similar situation naturally prevails with respect to λ and k^0 in the use of the Marcus–Hush model. Thus, a significant level of departure from reversibility is needed to determine k^0 and λ (or k^0 and α).

With FT-ac voltammetry, curve fitting providing excellent simulation-experiment comparisons over a series of harmonics and/or frequencies needs to be generated with a single combination of k^0 and λ (as well as other relevant experimental parameters) as required to confirm compliance to the Marcus–Hush model. Almost certainly, if just a single ac harmonic were computed using the Marcus–Hush model, but analysed by the

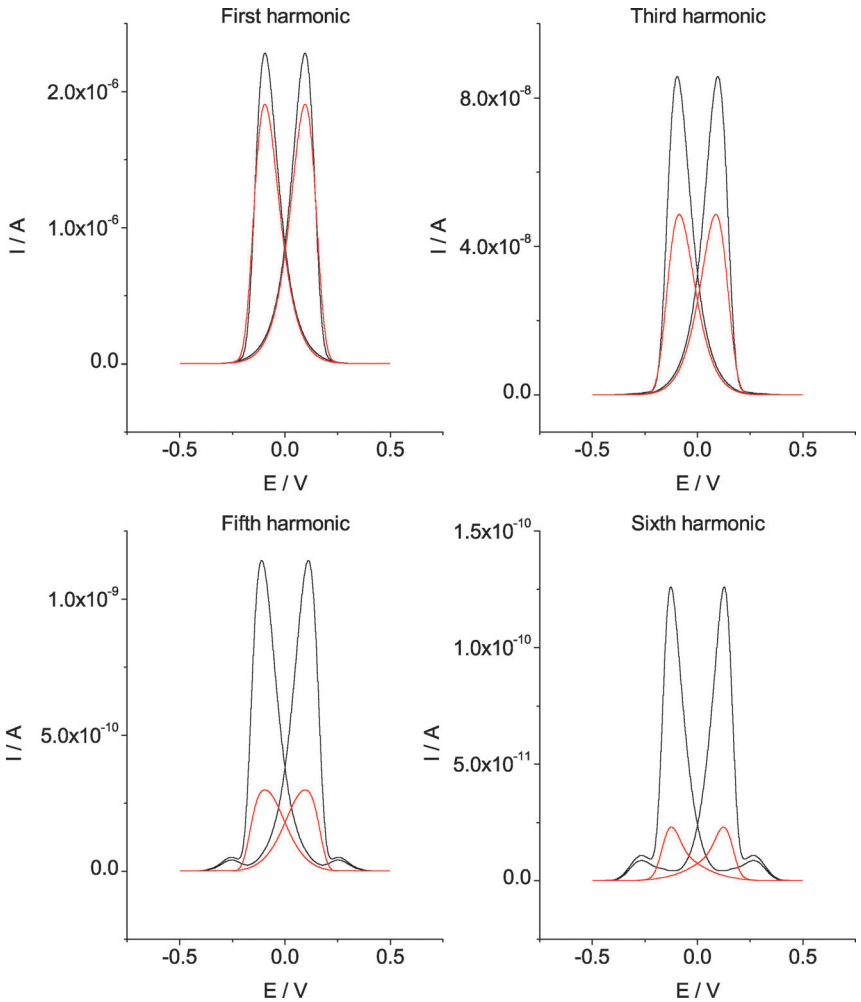

Fig. 8 Numerically simulated FT-ac harmonic data using parameter-set taken from.[12] Black line indicates Butler–Volmer theory with $\alpha = 0.5$ and $k_0 = 1.25\ s^{-1}$. Red line indicates Marcus–Hush theory with $\lambda = 0.85$ eV and $k_0 = 1.295\ s^{-1}$. Other parameters: $a = 0.7\ cm^2$; $E^0 = 0$ V; $C_{dl} = 0$ F cm^{-2}; $R_u = 0\ \Omega$; $T = 298$ K; and at $t = 0$ s, $\Gamma_A = 9.5$ pico-mol cm^{-2} and $\Gamma_B = 0$ pico-mol cm^{-2}; $f = 30$ Hz; $\Delta E = 0.05$ V; and $v = 0.5$ V s^{-1}.

Butler–Volmer model, then a combination of k^0 and α (= 0.5) would also fit the experimental data. However, a key feature to recognise is that these particular parameters would not lead to good fit for all the other harmonics. The challenge is to have experimentalists routinely fit data with the Marcus–Hush model to assess whether a significant data base encompassing many electrode processes can ultimately be established where this model is preferable. As Oldham advises,[34] the jury is still out on the need, or otherwise, for routine implementation of theoretical models based on Marcus–Hush theory as an alternative to the Butler–Volmer formalism. The critical question is to establish how to ascertain which model provides the better fit to experimental data.

6 Distinguishing the Butler–Volmer and Marcus–Hush models

In order to partially address the question as to what conditions are needed to allow the Butler–Volmer and Marcus–Hush theories to be distinguished, FT-ac voltammetric data obtained from simulations using the Butler–Volmer model were fitted to the Marcus–Hush model and *vice versa* for a single electron transfer reaction, eqn (1), under surface-confined conditions. The protocol used in this exercise, is when fitting Butler–Volmer model to Marcus–Hush simulation, the rate constant k^0 and α are varied to establish the level of fit available with the "wrong" model. Conversely, when fitting Marcus–Hush to Butler–Volmer derived data, k^0 and λ are varied.

In these fitting exercises, two simulations are made for each of the electron transfer theories; one where we expect the alternative theory may be able to achieve a good fit and one where we expect a good fit to be impossible. For the simulated data generated with Butler–Volmer theory, k^0 was fixed at $10\ s^{-1}$ and α was given a value of 0.4 or 0.5. With the first α value, use of the Chidsey formalism based on the Marcus–Hush theory is not expected to be able to adequately fit the simulated data,[13–15] while with $\alpha = 0.5$, this may be possible. With $\alpha = 0.4$, it is anticipated that the asymmetric Marcus–Hush theory[13–18] would have to be introduced to provide a satisfactory fit.

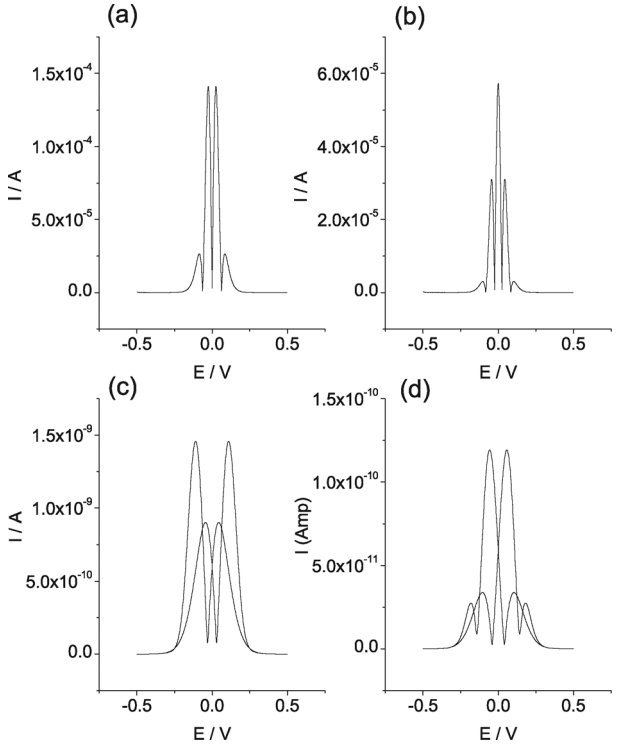

Fig. 9 (a) Fourth and (b) fifth FT-ac harmonic data for the diffusional model with Marcus–Hush electron transfer kinetics and parameters: at t = 0 s, Γ^* = 10^{-6} mol cm^{-3} and D = 2.310^{-5} cm^2 s^{-1}; k_0 = 100 cm s^{-1}. (c) Fourth and (d) fifth FT-ac harmonic data for the surface-confined model given in this work with Marcus–Hush electron transfer kinetics and parameters: at t = 0 s, Γ_A = 9.5 pico-mol cm^{-2} and Γ_B = 0 pico-mol cm^{-2}; k_0 = 1 s^{-1}. Other parameters: a = 1 cm^2; E^0 = 0 V; C_{dl} = 0 F cm^{-2}; R_u = 0 Ω; T = 298 K; λ = 0.25 eV f = 60 Hz; ΔE = 0.05 V; and v = 0.5 V s^{-1}.

For the simulated data generated with Marcus–Hush theory k^0 = 10 s^{-1} is again used and the parameter λ is either 0.1 eV or 1.0 eV. The expectation is that superior Butler–Volmer fits with α = 0.5 are likely to be achieved with the larger λ value.

The scenarios where Butler–Volmer and Marcus–Hush theories of electron transfer are unlikely to be distinguished are when Butler–Volmer has α = 0.5 and when Marcus–Hush has $\lambda \rightarrow \infty$ or the process is reversible, as can be seen by inspection of data in Fig. 1.

For simplicity, all simulations in this exercise are again conducted with R_u = 0 Ohm, C_{dl} = 0 Farad. Examples given are based on a single sine wave with ΔE = 100 mV, f = 200 Hz added to the dc ramp (scan rate = 1 V s^{-1}). It should also be noted that no account of double layer correction for electrode kinetics[10] is introduced into this analysis. This phenomenon provides a potential dependent term and hence may apparently mimic deviations from α = 0.5 that can be reported with the Butler–Volmer model.

The quality of fit (say Marcus–Hush model simulated with k^0 = 5 s^{-1} and λ = 1 eV) to a given data set (say Butler–Volmer model generated with k^0 = 10 s^{-1} and α = 0.5) may be judged using the least-squares method. The range of searching for this best fit is restricted to $0 \leq k^0/s^{-1} \leq 20$ and $0 \leq \lambda/eV \leq 20$ for the Marcus–Hush model and $0 \leq k^0/s^{-1} \leq 20$ and $0 \leq \alpha \leq 1$ for the Butler–Volmer model. Irrespective of the model used, for each pair of values a probability of that pair being correct relative to all other pairs of values was constructed. The details of this form of data analysis will be presented in an upcoming paper. For our purposes it is sufficient to know that the probability is inversely proportional to the least-squares value determined by comparing the fit to the original data simulated with the other electron transfer model. Note that this procedure does not change the best fit values when comparing these models, it is used as a convenient way of calculating error bars for these best fit values. The error bars can then be determined by summing up adjacent parameter pairs until the cumulative probability reaches 68.3%, and therefore gives the 1σ value.

The best fit parameter values and associated errors are shown in Table 1 for all fits of Marcus–Hush to Butler–Volmer (top) and Butler–Volmer to Marcus–Hush (bottom). As expected,

Table 1 Best fits for each data set considering each dc and ac harmonic components independently. Best fits for each of the dc and ac harmonic components data obtained from simulation using the Butler–Volmer model as fitted to by Marcus–Hush model and *vice versa*. High error bars and/or physically unlikely fits (such as α = 0.0) indicate where the fit is very poor. Also note that where $\lambda \geq$ 20 eV this indicates that the best fit for the Marcus–Hush model was limited by the restricted range for λ

MH fit to BV with α = 0.5			MH fit to BV with α = 0.4		
Harmonic	k^0_{fit} (s^{-1})	λ_{fit} (eV)	Harmonic	k^0_{fit} (s^{-1})	λ_{fit} (eV)
DC	10.2 ± 1.4	≥ 20.0 ± 7.9	DC	18.5 ± 7.9	0.5 ± 9.3
1	10.2 ± 1.6	≥ 20.0 ± 7.9	1	13.7 ± 5.3	1.3 ± 8.9
2	10.1 ± 2.4	≥ 20.0 ± 7.8	2	13.2 ± 5.2	3.7 ± 7.7
3	0.1 ± 3.0	≥ 20.0 ± 7.8	3	14.4 ± 6.0	18.4 ± 9.2
4	10.1 ± 3.5	≥ 20.0 ± 7.7	4	15.3 ± 6.7	20.0 ± 9.2
BV fit to MH with λ = 1.0 eV			**BV fit to MH with λ = 0.1 eV**		
Harmonic	k^0_{fit} (s^{-1})	α_{fit}	Harmonic	k^0_{fit} (s^{-1})	α_{fit}
DC	6.7 ± 5.9	0.5 ± 0.23	DC	0.2 ± 9.2	0.21 ± 0.35
1	7.2 ± 5.5	0.5 ± 0.22	1	2.1 ± 7.7	0.00 ± 0.43
2	7.9 ± 6.1	0.5 ± 0.23	2	0.1 ± 7.9	0.13 ± 0.29
3	0.7 ± 11.1	0.16 ± 0.31	3	0.2 ± 7.5	0.00 ± 0.31
4	0.5 ± 10.3	0.11 ± 0.30	4	0.1 ± 8.0	0.00 ± 0.31

the data simulated with Butler–Volmer with $\alpha = 0.5$ and $k^0 = 10\ s^{-1}$ was best fitted using Marcus–Hush theory with $k^0 = 10.2\ s^{-1}$ and $\lambda \rightarrow \infty$ (actually restricted to be $\lambda = 20$ eV in this example). Also as expected, simulations based on the Marcus–Hush model were unable to properly fit the Butler–Volmer data with $\alpha = 0.4$.

The Butler–Volmer fits to data generated by Marcus–Hush theory also behave as expected. Data in Table 1 show that for the dc and first two harmonics that Butler–Volmer model fits to Marcus–Hush simulated data with $\lambda = 1$ eV give the expected answer, while those simulated with $\lambda = 0.1$ eV give very poor fits with very large error bars.

Of great interest are the best fits and their errors obtained with different harmonics. This is particularly evident for the Marcus–Hush fits to the Butler–Volmer simulated data with $\alpha = 0.5$ compared to $\alpha = 0.4$ where the error bars for k^0 and λ encompasses the entire range (between 0 and 20). The sensitivity of the higher harmonics is strongly seen in the Butler–Volmer fits to the Marcus–Hush data, even when $\lambda = 1$ eV.

In practice, the systematic approach recommended for fitting to FT-ac voltammetric data is to show that the same parameters predict the best fit for all ac harmonics. If the "wrong" model is used the apparently best fit is harmonic dependent. The results given in Table 1 reveal that when Marcus–Hush simulation data are fitted to the Butler–Volmer generated data then the best fit is approximately harmonic independent. In contrast, when Butler–Volmer model is applied to the Marcus–Hush generated data, the best fit to each harmonic gives quite different k^0 and α values.

7 Conclusions

Simulations based on Marcus–Hush theory for electrode kinetics have been introduced into FT-ac voltammetry as a more fundamental alternative to Butler–Volmer theory employed in earlier studies. Systematic analysis of the harmonic component allows a distinction in the theoretical predictions to be achieved, providing the process is not too close to reversible. Thus, while predictions based on Marcus–Hush and Butler–Volmer relationships are essentially indistinguishable under many dc voltammetric conditions, the higher harmonics produced in large amplitude ac voltammetry may exhibit far greater differences. In principle, varying the frequency, f, induces different behaviour when using the Marcus–Hush or Butler–Volmer formalisms. If f is increased sufficiently, then the peak heights in the ac harmonics tend to a constant value when the underlying theory is based on Butler–Volmer kinetics, whereas they tend to zero when using Marcus–Hush kinetics. This, and analysis of the high order harmonics, should facilitate a better method for distinguishing the appropriateness of either model, therefore enabling predictions to be more readily made as to whether Butler–Volmer or Marcus–Hush theory should be invoked.

Finally, it should be noted that there is no greater complexity in the inverse problem in using symmetric Marcus–Hush theory as opposed to Butler–Volmer theory, since only two parameters are required for each formalism: Butler–Volmer uses k^0 and α; Marcus–Hush uses k^0 and λ. However, in cases where use of α is not equal to 0.5 have been apparently established from Butler–Volmer analysis, then no reasonable fit will be available with the Chidsey formalism. In this case, double layer electrode kinetic effects or introduction of an asymmetric Marcus–Hush model[13–18] will need to be considered. The FT-ac voltammetric method of analysis introduced in this work, seeks, as is the case in the very recent papers by Compton *et al.*,[13–18] to optimise the ability to detect often subtle distinctions available in the Butler–Volmer and Marcus Hush theories. Further work is now required to ascertain whether FT-ac, dc or square wave[13–18] or other methods achieve the maximum sensitivity with respect to addressing this issue.

Acknowledgements

The authors thank the Australian Research Council and EPSRC for financial support of this project. Extensive and valuable discussions with Dr Stephen Feldberg are also gratefully acknowledged. The work described in this paper is derived from the D.Phil. Thesis of G. P. Stevenson, St. Hugh's College, University of Oxford, 2010 and presented in part at the RSC/SCI Electrochemical Horizons Conference, Dublin, Ireland, September 4 to 6, 2012.

References

1 R. A. Marcus, *J. Chem. Phys.*, 1956, **24**, 966–978.
2 R. A. Marcus, *Annu. Rev. Phys. Chem.*, 1964, **15**, 155–196.
3 R. A. Marcus, *J. Chem. Phys.*, 1965, **43**, 679–701.
4 R. A. Marcus, *Electrochim. Acta*, 1968, **13**, 955–1004.
5 R. A. Marcus and N. Sutin, *Biochim. Biophys. Acta*, 1985, **811**, 265–322.
6 R. A. Marcus, *Angew. Chem., Int. Ed. Engl.*, 1993, **32**, 1111–1222.
7 N. S. Hush, *J. Chem. Phys.*, 1958, **28**, 962–972.
8 N. S. Hush, *Electrochim. Acta*, 1968, **13**, 1005–1023.
9 N. S. Hush, *J. Electroanal. Chem.*, 1999, **470**, 170–195.
10 A. J. Bard and L. R. Faulkner, *Electrochemical Methods*, Wiley, New York, 2nd edn, 2001.
11 V. G. Levich, *Adv. Electrochem. Electrochem. Eng.*, 1966, **4**, 249–371.
12 C. E. D. Chidsey, *Science*, 1991, **251**, 919–922.
13 E. Laborda, M. C. Henstridge and R. G. Compton, *J. Electroanal. Chem.*, 2012, **667**, 48–53.
14 M. C. Henstridge, E. Laborda, Y. Wanga, D. Suwatcharaa, N. Reesa, A. Molinab, F. Martínez-Ortiz and R. G. Compton, *J. Electroanal. Chem.*, 2012, **672**, 45–52.
15 M. C. Henstridge, E. Laborda and R. G. Compton, *J. Electroanal. Chem.*, 2012, **674**, 90–96.
16 D. Suwatchara, M. C. Henstridge, N. V. Rees, E. Laborda and R. G. Compton, *J. Electroanal. Chem.*, 2012, **677**, 120–126.
17 E. Laborda, M. C. Henstridge and R. G. Compton, *J. Electroanal. Chem.*, 2012, **681**, 96–102.
18 D. Suwatchara, N. V. Rees, M. C. Henstridge, E. Laborda and R. G. Compton, *J. Electroanal. Chem.*, 2012, **685**, 53–62.
19 D. J. Gavaghan and A. M. Bond, *J. Electroanal. Chem.*, 2000, **480**, 133–149.
20 D. J. Gavaghan, D. Elton, K. B. Oldham and A. M. Bond, *J. Electroanal. Chem.*, 2001, **512**, 1–15.
21 D. J. Gavaghan, D. Elton and A. M. Bond, *J. Electroanal. Chem.*, 2001, **513**, 73–86.
22 A. Anastassiou, K. Parker and D. O'Hare, *Anal. Chem.*, 2005, **77**, 3357–3364.
23 J. Garland, C. Pettit and D. Roy, *Electrochim. Acta*, 2004, **49**, 2623–2631.
24 D. E. Smith, *Anal. Chem.*, 1976, **48**, 221A–240A.
25 D. E. Smith, *Anal. Chem.*, 1976, **48**, 517A–526A.
26 D. E. Smith, in *Electroanalytical Chemistry*, ed. A. J. Bard, Marcel Dekker, New York, 1966, ch. 1.
27 D. E. Smith and H. H. Bauer, *CRC Crit. Rev. Anal. Chem.*, 1971, **2**, 247–343.

28 M. Overton, L. Alber and D. Smith, *Anal. Chem.*, 1975, **47**, 363A–374A.
29 L. T. Calcaterra, G. L. Closs and J. R. Miller, *J. Am. Chem. Soc.*, 1983, **105**, 670–672.
30 G. L. Closs and J. R. Miller, *Science*, 1988, **240**, 440–447.
31 T. T.-T. Li and M. J. Weaver, *J. Am. Chem. Soc.*, 1984, **106**, 6107–6108.
32 L. Tender, M. T. Carter and R. W. Murray, *Anal. Chem.*, 1994, **66**, 3173–3181.
33 S. W. Feldberg, *Anal. Chem.*, 2010, **82**, 5176–5183.
34 K. B. Oldham and J. C. Myland, *J. Electroanal. Chem.*, 2011, **655**, 65–72.
35 D. J. Gavaghan and A. M. Bond, *J. Electroanal. Chem.*, 2006, **18**, 333–344.
36 K. W. Morton and D. F. Mayers, *Numerical Solution of Partial Differential Equations*, Cambridge University Press, Cambridge, 1994.
37 B. Timmer, M. Sluyters-Rehbach and J. H. Sluyters, *J. Electroanal. Chem.*, 1967, **14**, 169–180.
38 A. M. Bond, *Broadening Electrochemical Horizons. Principles and Illustration of Voltammetric and Related Techniques*, OUP, Oxford, 2002.
39 D. E. Smith and T. McCord, *Anal. Chem.*, 1968, **40**, 474–481.
40 A. M. Bond, N. W. Duffy, S. Guo, J. Zhang and D. Elton, *Anal. Chem.*, 2005, **77**, 186A–195A.